Genome-Wide Differences in DNA Methylation Changes in Two Contrasting rapeseed Genotypes in Response to Drought Conditions

Dongfang Cai, Jiacheng Zhu, Jianping Wang, Junping He, Jinhua Cao, Yancheng Wen, Lei Zhao, Dongguo Wang, Shufen Zhang

Industrial Crops Research Institute, Henan Academy of Agricultural Sciences, Zhengzhou, Henan, China

Abstract

DNA methylation, which is one of the most important epigenetic modifications, has been found to affect various biological processes. Here, we studied the genome-wide DNA methylation changes using a pair of drought-tolerant and drought-sensitive *Brassica napus* varieties under drought and control conditions. Similar genome-wide DNA methylation levels were observed between two varieties, with an average of 34.99% CG, 23.42% CHG, and 41.59% CHH, respectively. We then analyzed the differential methylated regions (DMRs) between two varieties, and detected 649 CG, 3,700 CHG, and 12,207 CHH DMRs, which contained a total of 8,465 DMR-related genes (DMGs). Enrichment analysis suggested that DMR-related genes mainly participated on plant hormone signal transduction and photosythese-antenna proteins, which is associated with the drought stress tolerance. Using RNA-seq data, we found the methylation levels of the genes in genebody regions had negative effects on gene expression levels in control and re-watering condition, and the correlation were disappeared in drought stress condition. Taken together, we presented a methylome map of two rapeseed genomes, and found a total of 45 DMR-related genes were associated with drought stress tolerance. Thus, our results indicate that DNA methylation changes affects the drought stress tolerance in rapeseed through the regulation of plant hormone and photosythese-related gene expression.

Results

DNA methylation patterns in different rapeseed genomic regions

Table 1 The results of raw data analyzation and comprision

Samples	Clean_Reads	Clean_Base(bp)	Unique_mapped	Mapped rate(%)	Conversion_rate(%)	CG(%) [a]	CHG(%)	CHH(%)
P287-CK	143,614,930	43,047,233,216	94525212	65.82	99.67	35.18	22.87	41.95
P287-DR	146,101,260	43,791,093,038	97334139	66.62	99.68	35.85	23.08	41.07
P287-RE	154,051,214	47,959,400,320	100350147	65.14	99.68	35.04	22.63	42.33
T88-CK	158,668,483	47,558,111,008	104764716	66.03	99.66	34.49	23.77	41.75
T88-DR	139,808,510	44,111,778,960	94280972	67.44	99.64	34.7	24.1	41.21
T88-RE	149,117,631	44,696,097,034	95791174	64.24	99.66	34.67	24.08	41.25

P287, the drought-resistant rapeseed genotype; T88, the drought-sensitive rapeseed genotype; CK, under the control condition; DR, under the drought condition; RE, under the re-watering condition.
a. Relative proportions of mCs in three sequence contexts (CG, CHG and CHH) of the genotypes P287 and T88 under the control, drought and re-watering conditions, respectively.

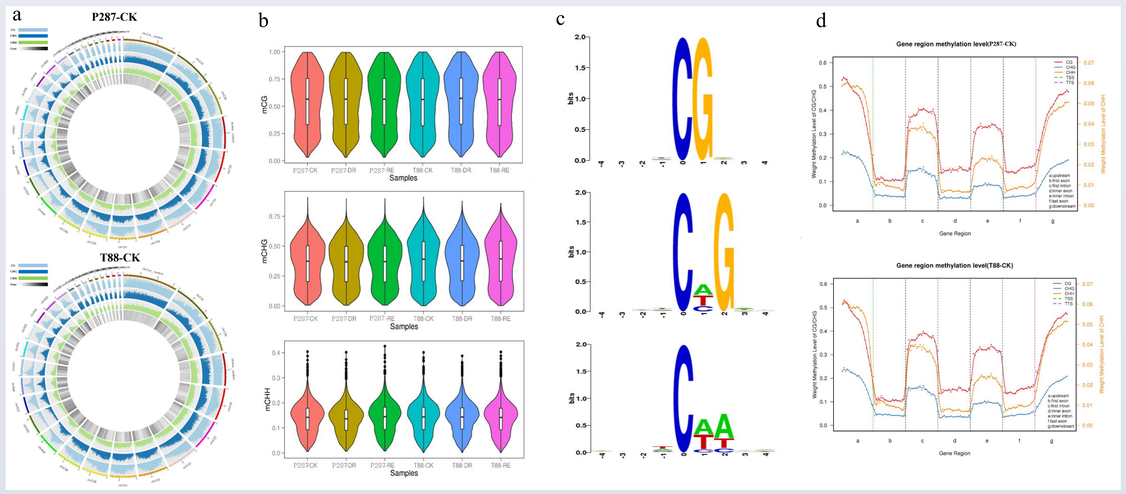

(a) Circos plots of chromosomes in rapeseed genome. The outermost three circles represented the methylation levels of 5mC in CG, CHG and CHH contexts, H = A, C or T. the inner circle represented the gene density of each chromosome. (b) Violin plot for the overall distribution of methylation levels in CG, CHG and CHH contexts, respectively. The horizontal axis represented six samples; the vertical axis represented the methylation levels of the samples; and the width of each violin represented the density of the point at that methylation level; while the boxplot shows the methylation levels in each violin. (c) Methylation preferences in 9 bp spanning CG, CHG, and CHH methylcytosine sites for the sample P287-CK. The horizontal axis was the base number order of the methylation site, the height of each base represented the relative frequency of the base at that position. (d) The weight methylation levels of the CG, CHG and CHH contexts in different gene functional regions. H = A, C or T. The horizontal axis represented the different functional regions of the gene that a, b, c, d, e, f, g denoted upstream, first exon, first intron, inner exon, inner intron, last exon and downstream, respectively. The left vertical axis represented the methylation levels of CG/CHG, and the right vertical axis represented the methylation levels of CHH. The dotted green and pink vertical line represented the transcription start site (TSS) and the transcription termination site (TTS), respectively. The red, blue and orange solid lines represent CG, CHG and CHH, respectively.

Identification of differentially methylated genes (DMGs) under control, drought and re-watering conditions

(a) Venn diagram of hyper/hypomethylated genes among the genotypes P287 and T88 under control, drought and re-watering conditions. (b) Heat maps of methylation levels of the CG, CHG and CHH DMGs in different gene functional regions, respectively. (c) KEGG pathway and GO enrichment analysis of hypermethylated genes in P287-CK_vs_P287-DR_T88-CK_vs_T88-DR. P287-CK_vs_P287-DR represented the comprision of P287-CK and P287-DR; T88-CK_vs_T88-DR represented the comprision of T88-CK and T88-DR; P287-CK_vs_P287-DR_T88-CK_vs_T88-DR represented the comprision of P287-CK_vs_P287-DR and T88-CK_vs_T88-DR . (d) KEGG pathway and GO enrichment analysis of hypomethylated genes in P287-CK_vs_P287-DR_T88-CK_vs_T88-DR. The size of the circle represented gene numbers, and the colour represented the q-value.

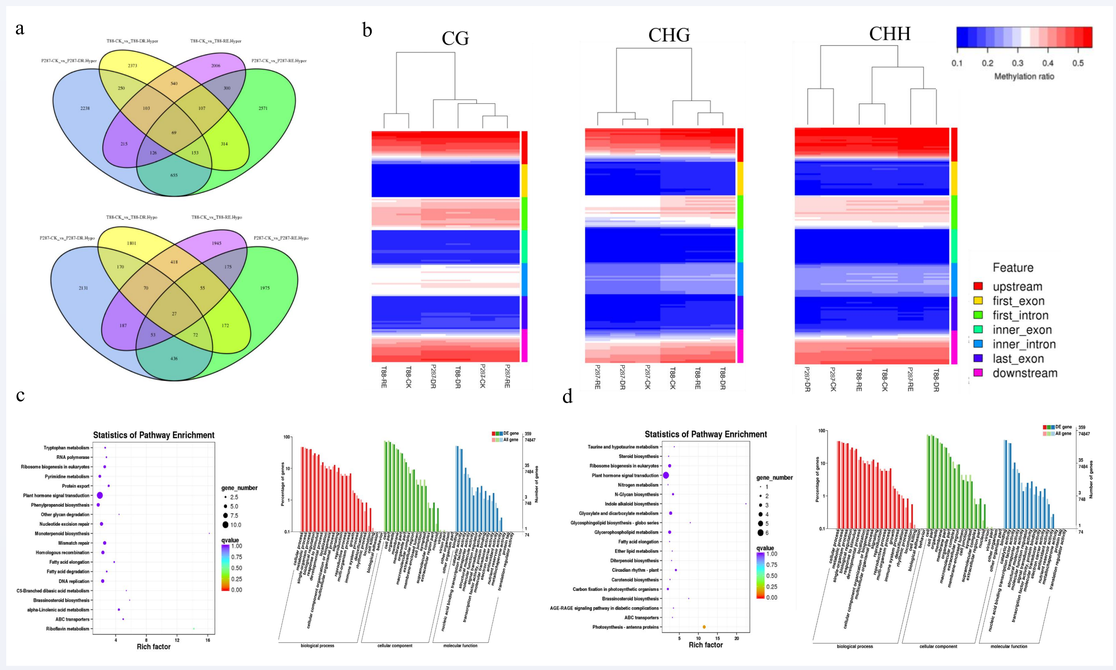

Correlation between DNA methylation status and gene expression levels

(a) The pearson correlation between the methylation levels of the all, CG, CHG and CHH mC sites and the expression levels in different gene functional regions. (b) The methylation levels of CG, CHG and CHH DMGs in different gene functional regions according to the divided four different degrees of expression levels. (c) The methylation levels of candidate genes of six samples in different functional region. The red, green and blue lines represented CG, CHG and CHH, respectively.

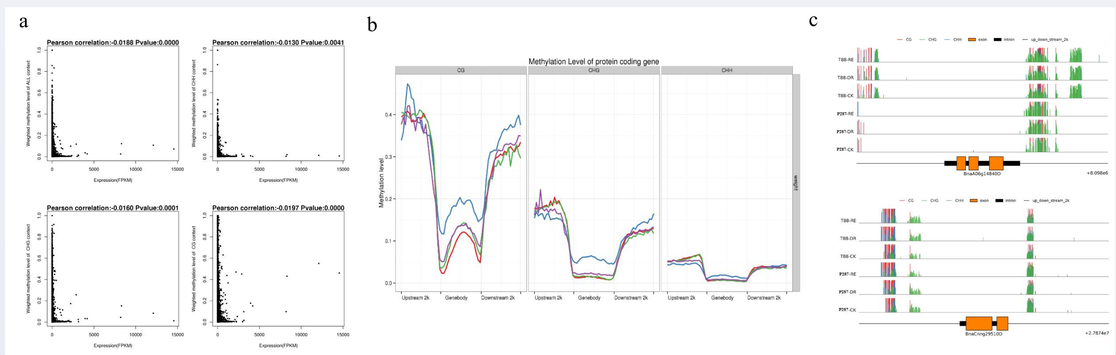

The identification of candidate genes and RT-PCR verification

Table 2 The annotation information of some candidate genes

Gene ID	Gene name	AGI number	Gene annotation	Notes
BnaC03g25160D		AT2G45180.1	Bifunctional inhibitor/lipid-transfer protein/seed storage 2S albumin superfamily protein	Related with salt, osmotic, cold stress
BnaC09g50580D		AT5G04470.1		Related with ROS stress
BnaA02g28870D		AT3G27350.2	transcriptional regulator ATRX-like protein;	
BnaA09g01080D	PSAD-1	AT4G02770.1		Related with drought stress
BnaA09g25210D		AT1G31350.1	KAR-UP F-BOX 1, KUF1	Related with abiotic stress
BnaA09g26570D		AT1G29910.1	photosynthesis, photosynthesis, light harvesting in photosystem I,	
BnaA09g29100D	ATHSP70, HSC70-4, HSP70	AT3G12580.1		Related with abiotic stress
BnaA10g03540D	AKS2	AT1G05805.1	regulation of stomatal movement,	
BnaAnng17910D	ATLEA14, LEA1, LEA14, LSR3	AT1G01470.1	response to wounding and light stress.	Related with salt and drought stress
BnaC05g31060D		AT1G76590.1	PLATZ transcription factor family protein	Related with abiotic stress
BnaC05g35990D		AT3G17520.1	LEA protein	Related with salt and drought stress
BnaC05g41830D	AHG3, ATPP2CA, PP2CA	AT3G11410.1	mRNA up-regulated by drought and ABA.	Related with salt, cold and drought stress
BnaC06g01610D	PGX3,	AT1G48100.1	carbohydrate metabolic process,	Related with salt and cold stress
BnaC06g15670D		AT3G55710.1	metabolic process	Related with defense reaction
BnaC06g29950D	ACR4	AT1G69040.2	regulation of cellular amino acid metabolic process,	
BnaC07g03450D	HBI1	AT2G18300.3	DNA-templated, response to cytokinin, response to hormone, transcription	Related with biotic and abiotic stress

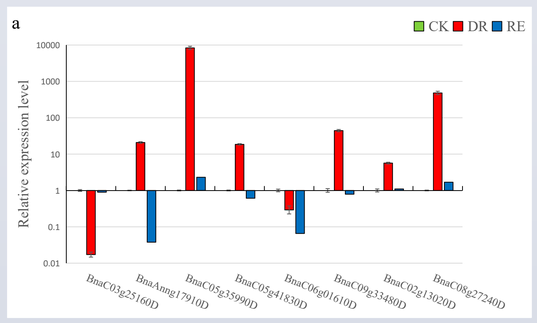

(a) The relative expression level of the selective eight candidate genes using real-time quantitative PCR (qRT-PCR) in the genotype P287 under the control, drought and re-watering conditions.

Conclusions

This study revealed the global DNA methylation patterns of rapeseed genome and widespread DNA methylation alteration under the water deficit stress. Our results demonstrated that DNA methylation may contribute to a better understanding of epigenetic regulation in adapting to the adverse environmental stresses, such as drought stress.

Acknowledgments

This work was funded by the National Key Technology Research and Development Program (Grant number 2018YFD0100600), the Special Project for Construction of Modern Agricultural Industrial Technology System (Grant number CARS-12) and the Outstanding Youth Foundation of the Henan Academy of Agricultural Sciences (Grant number 2018YQ06).